PCCP

Accepted Manuscript

ROYAL SOCIETY OF CHEMISTRY

www.rsc.org/pccp

Cite this: DOI: 10.1039/c0xx00000x

www.rsc.org/xxxxxx

ARTICLE TYPE

Organosilane-Functionalized Graphene Quantum Dots and Their Encapsulation into Bi-Layer Hollow Silica Spheres for Bioimaging Application

Ting Wen,[‡] Baocheng Yang,[‡] Yanzhen Guo, Jing Sun, Chunmei Zhao, Shouren Zhang, Miao Zhang, and Yonggang Wang*

Received (in XXX, XXX) Xth XXXXXXXXX 20XX, Accepted Xth XXXXXXXXX 20XX
DOI: 10.1039/b000000x

Graphene quantum dots (GQDs) represent an important class of luminescent quantum dots owing to their low toxicity and superior biocompatibility. Chemical functionalization of GQDs and subsequent combination with other materials further provide attractive techniques for advanced bioapplications. Herein, we report the facile fabrication of fluorescent organosilane-functionalized graphene quantum dots (Si-GQDs) and their embedding into mesoporous hollow silica spheres as biolabel for the first time. Well-proportioned Si-GQDs with bright and excitation dependent tunable emissions in the visible region were obtained via a simple and economical solvothermal route adopting graphite oxide as carbon source and 3-(2-aminoethylamino)-propyltrimethoxysilane as surface modifier. The as-synthesized Si-GQDs can be well dispersed and stored in organic solvents, easily manufactured into transparent film and bulk form, and particularly provide great potential to be combined with other materials. As a proof-of-principle experiment, we demonstrate the successful incorporation of Si-GQDs into hollow mesoporous silica spheres and conduct preliminary cellular imaging experiments. Interestingly, the Si-GQDs not only serve as fluorescent chromophore in the composite material, but also play a crucial role in the formation of mesoporous hollow silica spheres with distinctive bi-layer architecture. The layer thickness and optical properties can be precisely controlled by simply adjusting the silane coupling agent addition procedure in the preparation process. Our demonstration of low-cost Si-GQDs and their encapsulation into multifunctional composites may expand the applications of carbon-based nanomaterials for future biomedical imaging and other optoelectronic applications.

Introduction

Luminescent carbonaceous nanomaterials, including carbon quantum dots (CQDs or CDs) and graphene quantum dots (GQDs), have aroused tremendous research interest owing to their unique properties such as outstanding optical properties, low cytotoxicity and superior resistance to photo-bleaching.[1-7] Unlike artificial CQDs usually with amorphous structure and unclear luminescence mechanism, GQDs derived from the typical 2D graphite structure exhibit definite optical and electronic properties that originated from quantum confinement and edge effects. These structure features make GQDs potential for further chemical manipulations for advanced applications in photovoltaic devices,[8-11] light emitting,[12] photocatalysis[13,14] and especially bioimaging.[4-6,15,16] Up to now, various techniques have been developed to prepare GQDs, such as the electron beam lithography,[17] electrochemical approach,[18,19] reoxidization[20,21], laser ablation[22] and organic synthesizing strategy.[23-25] However, these top-down or bottom-up methods often involve complex processes and severe synthetic conditions with low productivity. In contrast, hydrothermal or solvothermal route which can cut peroxidized graphene sheets into ultrafine graphene pieces with diameters below 100 nm is an alternative approach to obtain large-scale and well-dispersive GQDs.[26-28] It is also a feasible way to obtain modified GQDs in one pot.[5,29]

Recent studies have shown that there are often carboxylic acid moieties at the surface of GQDs, which endows them possibility for subsequent modifications with organic, polymeric, inorganic or biological species. Chemical modification of GQDs is getting more attentions owing to their distinct effects on emission efficiency enhancement,[29-31] spectrum regulation[4,12,33,33] and functionalization.[34] With strong electron donating or withdrawing ability, the modifiers can improve the optical properties through drastic impact on electronic characteristics of conjugated structure of carbon, including hydroxyl compounds, dimethyl formamide, amines.[4,5,12,21,29] Primary amines as typical strong electron donors were firstly applied in the modification of carbonaceous luminescent materials as passivants[35] and had been certified to improve the emission efficiency effectively.[29] In some recently reported modifications of carbonaceous luminescent materials, primary amino-organosilanes were adopted as bifunctional modifiers and shown great potential for the design of luminescent carbonaceous materials of extended applications. For example, when 3-aminopropyl trimethoxysilane (APTMS) was used as both carbon source and surface modifier, hydrophilicity and temperature-sensitivity of individual Si-CQDs could be achieved simultaneously.[36] The products, luminescent Si-CQDs films, were proved to have great potential in the fabrication of temperature-sensitive devices. In another work, organosilane-functionalized CQDs were fabricated using N-(β-aminoethyl)-γ-aminopropyl methyldimethoxy silane (AEAPMS) as coordinating solvent, which can greatly enhance the loading proportion of

CQDs into silica matrices.[34,37] Then the organosilane-functionalized CQDs were applied in the preparation of fluorescent silica sol for bioimaging and hybrid luminescent gel glasses for photonics and optoelectronics devices. However, in these methods, the use of large-amount expensive organosilanes as solvent or carbon source is uneconomical. It is necessary to develop a new strategy to use primary amino organosilanes as little as we can and more effectively.

Encapsulation of toxic semiconductor quantum dots into biocompatible composites currently is a hot topic of nanomaterial science. Whereas, embedding CQDs/GQDs into other composite materials is seldom reported to the best of our knowledge. A recent work by Biswal *et al.* has demonstrated the encapsulation of GQDs inside ZIF-8 nanocrystals.[38] Tailoring of the photoluminescence and prominent stabilization of GQDs are observed together with increased water adsorption capacity. It is conceivable that further investigations to combine CQDs/GQDs with other functional materials can provide more composite materials with extraordinarily optimized luminescence and multifunctionality. Herein, we use organosilane 3-(2-aminoethylamino) propyltrimethoxysilane (AEAPTMS) as a "*one-stone-two-birds*" surface modifier to prepare organosilane-functionalized graphene quantum dots (Si-GQDs) and then demonstrate their encapsulation into hollow mesoporous silica spheres. A one-step solvothermal route is established to produce highly luminescent Si-GQDs with typical excitation-dependent behaviour. Organosilanes located at the surface of GQDs fastened the attachment of the GQDs to silica, and then avoided the fluorescence attenuation caused by fluorescein leading. The obtained fluorescent hollow mesoporous silica spheres (FHMSSs) present a distinctive bi-layer structure. The thickness of inner layer and the fluorescence intensity of FHMSSs can be simultaneously controlled by adjusting the addition amount of AEAPTMS. Finally, the luminescent FHMSSs were massively produced and applied in primary cellular imaging experiments. Our work provides an affordable route to luminescent Si-GQDs which show great potential in combination with other compositions for advanced bioimaging applications.

Materials and methods

Synthesis of graphene oxide (GO)

Graphite oxide was prepared from natural graphite powder by the modified Hummers method.[39] Firstly, 1.0 g Graphite powder and 4.5 g $KMnO_4$ was added into a mixture of concentrated H_2SO_4/H_3PO_4 (90/10 mL) under stirring. Then the reactants were heated to 50 °C and kept at this temperature for 12 hours. The suspension turned to golden yellow when 1 mL H_2O_2 (30% wt) was added. Then it was centrifuged (5000 rpm for 20 min), and the supernatant was decanted away. The remaining solid material was then washed with distilled water and HCl (30% wt) for several times, and then freeze-dried under vacuum overnight.

Synthesis of organosilane-funcionalized graphene quantum dots (Si-GQDs)

3-(2-Aminoethylamino)propyltrimethoxysilane (AEAPTMS) was mixed with ethanol to a final concentration of 0.05 M and a volume of 10 mL. 0.2 g GO was dispersed in the solution under ultrasonic condition. The suspension was heated hydrothermally in a 25 mL stainless-steel autoclave at 150 °C for 10 h. The resulting light-yellow solution was cooled to ambient temperature and centrifuged at 15000 rpm for 20 min. The supernatant was collected and purified with a RC membrane (MWCO = 1 kD) in ethanol for 24 h. Then the transparent, light-yellowish solution was concentrated to 10 mL by a rotary evaporator with the Si-GQDs concentration of 12.5 mg mL^{-1}. The final solution containing Si-GQDs were stable for at least 10 months.

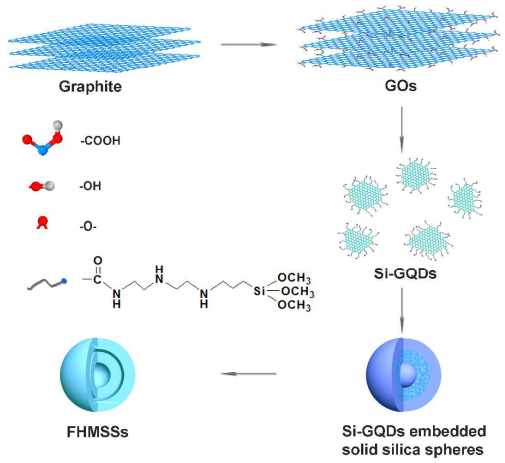

Scheme 1. Fabrication process of the fluorescent hollow mesoporous silica spheres. Only those silane groups on the edge of Si-GQDs are drawn for clearance. For more details, see discussions in the main text.

Synthesis of Si-GQDs embedded solid silica spheres

Si-GQDs embedded solid silica spheres were synthesized by using a modified Stöber method.[40] In a typical synthesis process, 6 mL tetraethylorthosilicate (TEOS) were rapidly added into a mixture of 80 mL ethanol and 20 mL ammonium aqueous solution (25-28%), and reacted for 1 min under vigorously stirring. Then a mixture of 8 mL as-prepared Si-GQDs solution (no Si-GQDs solution addition in the controlled trials) and 25-250 μL AEAPTMS was added into the reaction suspension dropwise and stirred for 1 h at room temperature. A solution of 4 mL TEOS in 16 mL ethanol was subsequently added dropwise into the reaction suspension and continued to react for 2 h. After that, the resulting silica particles were separated by centrifugation (9000 rpm for 3 min) and washed with distilled water and ethanol. The obtained solid was dried overnight at 60 °C. 2.9 g of the final product can be obtained from 0.2 g GO and 6 mL TEOS.

Synthesis of fluorescent hollow mesoporous silica spheres (FHMSSs)

FHMSSs were obtained following a cationic surfactant assisted selective etching strategy.[41] The overall synthesis process was provided in **Scheme 1**. 50 mg of the as-prepared solid silica spheres were dispersed thoroughly in 9 mL (9.5 mL in the controlled trials) deionized water under ultrasonication for 15 min. 1 mL cetyltrimethyl ammonium bromide (CTAB) aqueous solution (12.5 mg mL^{-1}, 0.5 mL in the controlled trials) was added into the suspension and stirred at room temperature for 30 min. Then 0.5 g Na_2CO_3 was added into the mixture and stirred at 45 °C for 24 h. The final products were collected by centrifugation and washed with distilled water and ethanol.

Synthesis process of hollow mesoporous silica spheres was the same as FHMSSs completely except no Si-GQD was added during the solid silica sphere preparation procedure.

Synthesis of Si-GQDs film and block

Si-GQDs film and block were prepared by dropping a mixture solution of Si-GQDs and AEAPTMS (1:2 v/v) on a glass or in a mould and dried in an oven (50 °C) until they were cured entirely. In the block case, the mould was removed after the Si-GQDs block was completely solidified.

Determination of the quantum yields (QY)

The QYs of the Si-GQDs were estimated by comparing their integrated PL intensities (excited at 360 nm) and absorbance at 360 nm with those of quininesulfate. Quinine sulfate (f = 0.54) was dissolved in 0.1 M H_2SO_4 (refractive index: 1.33) and the Si-GQDs were dissolved in ethanol (refractive index: 1.36). To minimize the self-absorption effect, the absorbance of each solution (in a 10 mm cuvette) at the excitation wavelength was adjusted less than 0.1. The excitation and emission slit widths were set at 2.5 nm when recording the PL spectra.

Cellular imaging

HePG2 cells were cultured in DMEM containing 10% fetal bovine serum, 100 U mL^{-1} penicillin, and 100 mg mL^{-1} streptomycin at 37 °C in 5% CO_2 and 95% air. 200 μg FHMSSs were added into 1 mL of DMEM medium containing HePG2 cells on a glass bottom dish (35 mm). The glass dish was washed three times with phosphate buffer after incubation 4 h at 37 °C.

Characterization

Scanning electron microscopy (SEM) and transmission electron microscopy (TEM) images were recorded using FEI Quanta-250 (20 kV) and FEI Tecnai-G2-20 with an accelerating voltage of 200 kV, respectively. Powder X-ray diffraction (PXRD) data of all the samples were collected at room temperature (25 °C) on a Bruker D8 Advance ECO diffractometer with Cu Kα radiation (λ = 0.15418 nm) under the tube conditions 40 kV and 40 mA. The low-angle X-ray diffraction patterns in the 2θ range of 1–5° were collected on the same instrument in a step of 0.01° and remaining time 1 s per step. Prior to XRD measurements, the Si-GQDs were placed on glass supports. Fourier transform infrared spectra (FTIR) were recorded on a Nicolet IS5 spectrometer as KBr pellets in the range of 400–4000 cm^{-1} with the spectral resolution of 2 cm^{-1}. A Malvern zetasizer 2000HS was used to measure the size of Si-GQDs. UV–Vis spectra were recorded by a Hitachi U-4100 UV-Visible-NIR spectrophotometer. All the samples were dispersed in ethanol in this measurement. The PL spectra of the Si-GQDs solution, Si-GQDs block and FHMSSs powder were recorded using a Hitachi F-4600 spectrophotometer. The Cellular images were taken with Nikon fluorescence microscope (Nikon Eclipse Ti-S, CCD: Ri1). The N_2 adsorption–desorption isotherms were determined at 77 K by a volumetric method with a Quadrasorb SI-MP.

Results and discussion

Fluorescent Si-GQDs were synthesized successfully via a simple top-down solvothermal route using graphite oxide as the carbon source and 3-(2-aminoethylamino) propyltrimethoxysilane as the surface passivation agent in ethanol (as shown in **Scheme 1**). **Figure 1** shows the TEM and high-resolution TEM (HRTEM) images of the as-prepared Si-GQDs. They are well-proportioned nanoparticles with a mean size of approximate 20 nm in diameter and about one or several nanometers in thickness according to previous investigations through similar synthetic route.[27,28,31] The HRTEM image of individual Si-GQDs shows clear lattice fringes with a *d* spacing of about 3.54 Å, which is consistent with the [002] facet of graphene and also indicates their single crystal nature.[4,20] The diameters of the Si-GQDs present a relatively broad distribution, ranging from 4 to 26 nm and giving an average value of 14.4 nm as derived from the dynamic light scattering (DLS) measurement result (**Figure 1c**). The particle size and morphology are comparable with those GQDs (with or without organosilane functionalization) reported previously by other research groups.[6,21,27,28,31] It's worth mentioning that the extremely low concentration (0.05 M) of expensive organosilane utilized makes our syntheses method affordable for large scale production and thus serving as one of the constituents of multifunctional composites. We also took powder XRD pattern of the Si-GQDs (as shown in **Figure S1**). The products through top-down methods with GO as starting material are always covered with various defects, which together with the small thickness result in broadened diffraction peak in the PXRD pattern. The broad band centered at about 24° is accordant with the characteristic lattice spacing of 3.52 Å of graphene.

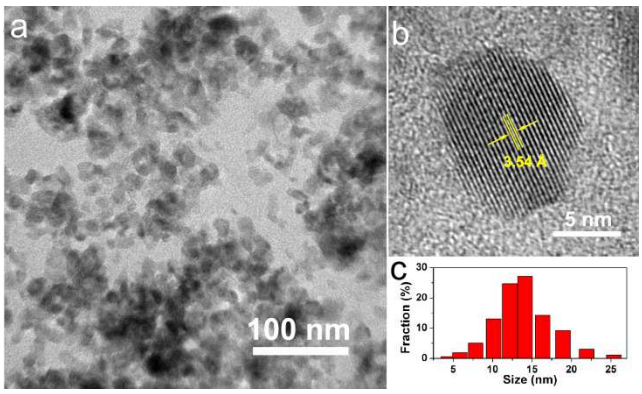

Fig. 1 (a) TEM image of the Si-GQDs; (b) high-resolution TEM image of an individual Si-GQD; (c) diameter distribution of the Si-GQDs.

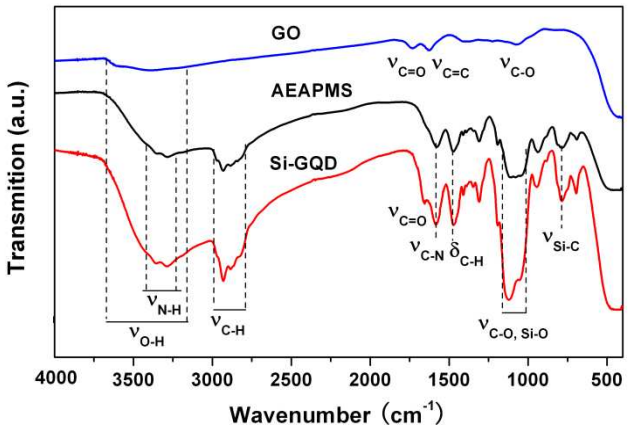

Fig. 2 FTIR spectra of the GOs, AEAPMS, and Si-GQDs.

FTIR spectra of the reactants (GOs, AEAPMS) and the final products are represented in **Figure 2** to reveal the organosilane groups on the surface and the formation mechanism of Si-GQDs. Under solvothermal conditions of both high temperature and spontaneous generated pressure, pyrolysis and acylation processes proceed successively. Firstly, the GOs were pyrolyzed into a mass of graphene fragments with carboxyl groups on their surface. And then *in situ* bonding between the fresh generated carboxyl groups and the primary amine moieties of AEAPTMS occurred adequately. Most of the FTIR peaks of AEAPTMS retain on that of Si-GQDs, while an emerging peak at 1656 cm^{-1} can be attributed to the connective bonding C=ONH between the organosilane and the GQDs. It is different from the C=OOH vibration peak of GOs at 1740 cm^{-1} and absent in the spectrum of AEAPTMS. In addition, the existence of C=ONH groups also can be verified by the C-NMR spectra, which shows a typical signal at chemical shift of 166 ppm as shown in **Figure S2**.

Figure 3 represents the absorption and photoluminescence spectra of GOs and Si-GQDs. The as-prepared Si-GQDs show bright blue luminescence under UV excitation. When excited at 360 nm, a strong emission band centered at 433 nm can be obtained, with a stocks shift of 73 nm (0.58 eV). In the UV-Vis absorption spectra, a marked difference is observed between GOs and Si-GQDs: the band of GOs at 222 nm is attributed to the typical π-π* transition of aromatic sp^2 domains, while the new band of Si-GQDs centered at 334 nm can be assigned to the n-π* transition. The aromatic structure on the edges of Si-GQDs combined with enthetic surface modificatory groups and further enlarged edges of Si-GQDs make the n-π* transition more possibly to happen compared with GOs. A further optical property of Si-GQDs is expected to show excitation-dependent photoluminescence behavior. As shown in **Figure 3b**, when excited under various excitation wavelengths, the Si-GQDs exhibit visible emissions with different peak intensities and centre positions, similarly as other carbon-based nanomaterials without surface modification. According to the *ab-initio* calculation results by Kumar *et al.*, newly created energy levels due to orbital hybridization can exist as interbands within the band gap in functionalized GQDs, which are considered responsible for excitation dependent tunable photoluminescence.[33] The strongest emission appears under the excitation of 360 nm and the PL quantum yield of 8.2% is obtained by using quinine sulfate as reference.

The as-synthesized Si-GQDs can be coated on a glass substrate straightway or solidified to form a firm bulk thanks to the numerous methoxy active groups on the particle surface acquired from AEAPTMS. Both the resulted Si-GQDs film and bulk exhibit bright blue emissions under commercial 365 nm UV lamp as shown in **Figure S3**. The fluorescence spectra of the bulk are comparable with that of Si-GQDs solution except a broaden excitation range from 320 nm to 520 nm which may be caused by the cumulation effect of Si-GQDs.

The active methoxy groups on the surface of Si-GQDs also endow them with the possibility to incorporate into the universal silica microspheres through Si-O bonding, which can provide a new route to achieve luminescent silica nanoparticles for bio-applications. In our study, the Si-GQDs hybridized silica spheres are prepared by a modified Stöber method[40] and the Si-GQDs blended with the silane coupling agent (AEAPTMS) are concentrated distributed in the interlayer between the core and outer layer of the silica spheres (see **Scheme 2**). Then the Si-GQDs embedded silica spheres are etched into FHMSSs with Na_2CO_3 through a "cetyltrimethylammonium cations (CTA^+)-promoted etching-redeposition" route.[42]

Figure 4 shows the morphology and photoluminescence properties of silica microspheres and the hybridized materials. Surprisingly, the obtained uniform silica spheres present a distinct bi-layer hollow structure, whereas the controlled trials without Si-GQDs addition bring marked different results that hollow or core-shell structure silica spheres can be obtained depending on the amount of silane coupling agent (see **Figure S4**). A wormhole-like mesostructrure is presented in the shell of FHMSSs (as shown in **Figure 4e**), indicating potential multipurpose applications such as drug delivery of these bifunctional microspheres in the future. The thickness of the inner layer of the FHMSSs increases with elevated amount of the coupling agent and the FHMSSs with thicker inner layer retains higher fluorescent intensity after the etching process (see **Figure S5**), indicating more Si-GQDs are fastened in the thicker inner layer. So we can come to a conclusion that both Si-GQDs and AEAPTMS are crucial in the formation process of the inner layer. The FHMSSs powders are white under natural light and exhibit bright blue emission under ultraviolet irradiation (365 nm). They show excitation-dependent PL behavior similar as that of pure Si-GQDs (**Figure S6a**).

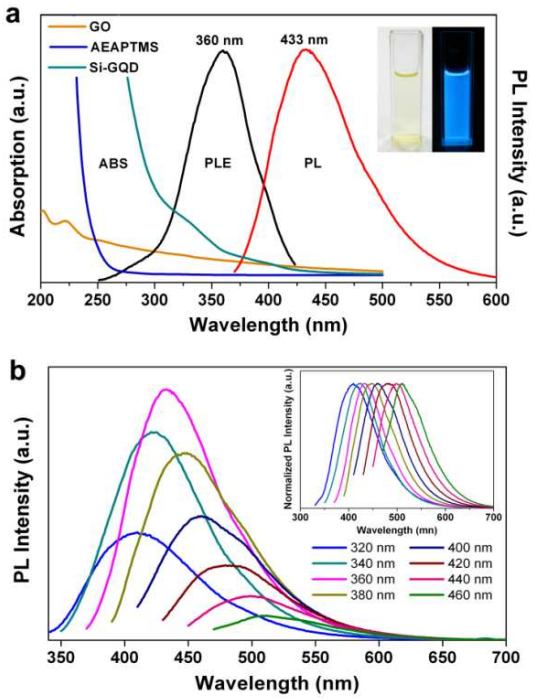

Fig. 3 (a) UV–Vis absorption (ABS, green), PLE and PL spectra of the Si-GQDs dispersed in ethanol; UV–Vis absorption (ABS, yellow) spectrum of GOs dispersed in ethanol; UV–Vis absorption (ABS, AEAPTMS) spectrum of GOs resolved in ethanol. Inset: Optical photographs of the Si-GQDs ethanol solution taken under visible light and ultra visible with wavelength of 365 nm; (b) PL emission spectra (recorded from 320 to 460 nm in 20 nm increments) of the Si-GQDs in ethanol. The normalized PL emission spectra are given as insert.

Cite this: DOI: 10.1039/c0xx00000x

www.rsc.org/xxxxxx

ARTICLE TYPE

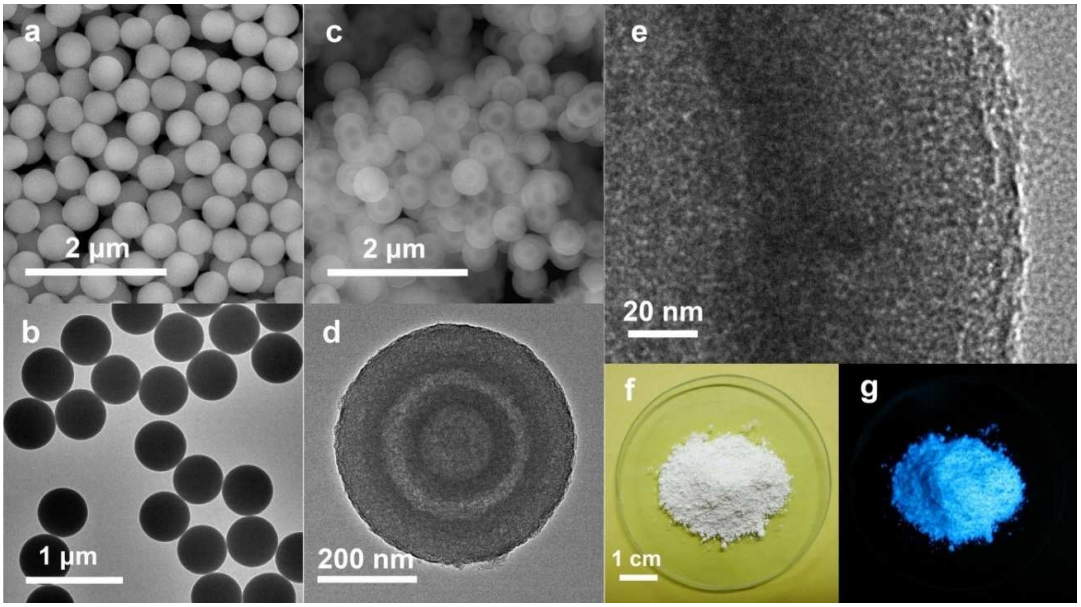

Fig. 4 (a, b) SEM and TEM images of Si-GQDs embedded solid silica spheres; (c) SEM image of FHMSSs; (d) TEM image of single FHMSS; (e) HRTEM image of the shell of the FHMSS; (f, g) Optical photographs of the FHMSSs powder taken under visible light and UV with wavelength of 365 nm.

As proposed in a "CTA^+-promoted etching-redeposition" route,[43] the formation mechanism of simple hollow mesoporous silica spheres is that cetyltrimethylammonium cations absorbed on the silica spheres surfaces can result positive charges to promote further etching by Na_2CO_3 and then soluble silicate species redeposite on the etched silica sphere surfaces together with CTA^+ clusters to form the mesoporous shells. According to this mechanism, we suppose that the formation of the interesting bi-layer structure is due to the uneven structure of Si-GQDs embedded silica spheres resulted by the complex texture of Si-GQDs and the silane coupling agent. As shown in **Scheme 2**, after the formation of the outer layer, the etching process is suspended by the compact complex of Si-GQDs with the silane coupling agent and thus tends to form a new surface. Then, CTA^+ absorbs on the new surfaces and the "CTA^+-promoted etching-redeposition" proceeds until the inner shell forms ultimately. To further testify this formation mechanism, a controlled trial with half of the CTA^+ concentration was conducted, where the dissolution of SiO_2 by Na_2CO_3 is much slower and no bi-layer structural hollow silica spheres were observed in 48 hours.

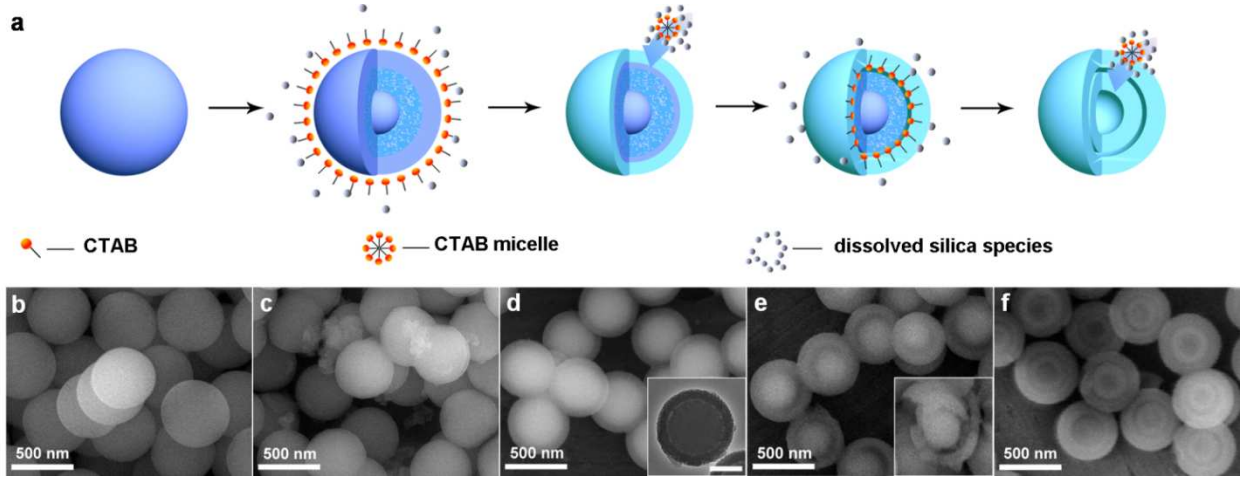

Scheme 2 (a) Schematic illustration for the etching process of FHMSSs; (b-f) SEM images of the etched products of Si-GQDs embedded solid silica spheres with AEAPTMS of 100 μL in 0 h, 2 h, 6 h, 12 h and 24 h. The inset in (d) is the TEM image of a single silica sphere in 6 h of the etching experiment and the bar stands for 200 nm.

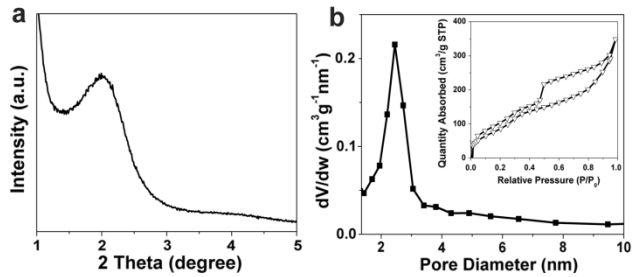

Fig. 5 (a) Low-angle X-ray diffraction pattern of FHMSSs; (b) Pore size distribution of FHMSSs derived by N_2 sorption isotherms (inset).

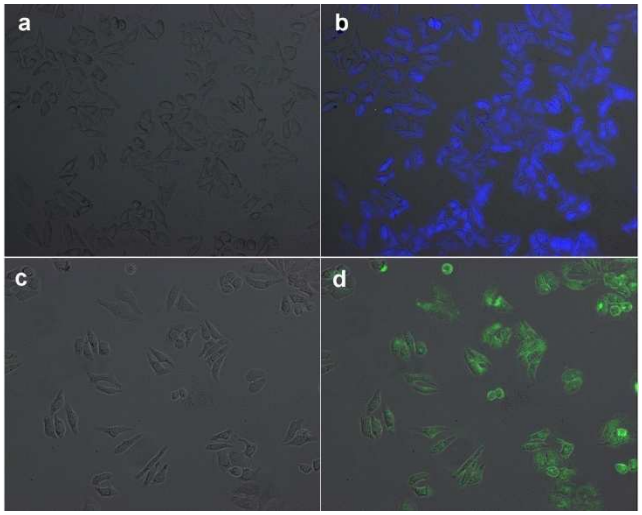

Fig. 6 (a, c) Cellular imaging of FHMSSs under bright field; (b, d) Merged images of cellular imaging of FHMSSs under 405 nm and 488 nm excitations, respectively.

Low-angle X-ray diffraction studies and N_2 adsorption-desorption measurements were conducted to further evaluate the mesoporous structure of FHMSSs. The results are presented in **Figure 5**. The broad diffraction peak at approximately $2\theta = 2.0°$ with *d* spacing 4.37 nm and a weak shoulder around 4.0° are typical for limited organized mesostructure.[42,43] After CTAB was removed by refluxing in NH_4NO_3/ethanol solution, the porosity of FHMSSs was investigated by N_2 adsorption-desorption measurements. The FHMSSs exhibit a type IV isotherm with a type H2 hysteresis loop, which indicates irregular pore shapes and size distribution of the mesoporous materials. The BET surface area of FHMSSs is calculated to be 344.7 $m^2\ g^{-1}$. FHMSSs has a narrow size distribution centered at about 2.5 nm and the pore volume of FHMSSs is 0.67 $cm^3\ g^{-1}$ as obtained from the BJH method shown in **Figure 5b**. The average pore wall thickness of 1.87 nm can be calculated according to both the *d*-spacing of the main diffraction peak from X-ray diffraction patterns and pore spacing from BET measurement.

Hollow mesoporous silica spheres (HMSSs) were extensively studied as vital drug delivery materials owing to their large surface area, high drug loading capacity, highly permeable porous shell and benign biocompatibility.[44-48] Benefit by the rewarding photoluminescence brought by Si-GQDs addition, the as-prepared FHMSSs are very promising to have extensional application in biomedical field. To demonstrate the luminescence performance of FHMSSs in potential bioapplications, preliminary *in vitro* cellular uptake experiments were performed in HePG2 cells. Cells were cultured and maintained in DMEM medium containing FHMSSs 200 μg mL^{-1}. As shown in **Figure 6**, confocal images of HePG2 cells incubated with FHMSSs at bright field and different excitation wavelengths show blue and green colors upon excitation at 405 nm and 488 nm, respectively. According to the merged images, FHMSSs were agglomerated mainly in the cell membrane and the cytoplasmic area leaves clear zones of nuclei. Additionally, no blinking or photobleaching was observed even after excitation for a prolonged time. These results suggest that the present FHMSSs possess of strong enough luminescence as promising material in the applications of bioimaging and biolabeling and can be easily imaged by conventional fluorescence microscopy. We wish this bifunctional material could be found more applications in future.

Conclusions

In conclusion, organosilane-funcionalized graphene quantum dots have been fabricated successfully through a simple solvothermal route adopting GOs as carbon resource and low concentration AEAPTMS (0.05 M) as the surface modifier. The as-obtained Si-GQDs show intense blue fluorescence under UV excitation (λ_{ex} = 360 nm) and a typical excitation-dependent emission behavior. Benefit from the marginal methoxysilyl active groups, the Si-GQDs can be easily processed into either a film on substrates firmly or solidified as a bulk, which endowed the Si-GQDs possibility for further bio-applications. We demonstrate the incorporation of Si-GQDs into hollow mesoporous silica spheres (FHMSSs) which can generate a distinctive bi-layer structure. The thickness control of the inner layer and photoluminescence enhancement can be achieved simultaneously by adjusting the silane coupling agent concentration. The blue- and green-emitting FHMSSs represent excellent performance in the preliminary cellular imaging tests. Our demonstration provides an affordable method for organosilane-functionalized GQDs as fluorescent component for subsequent multifunctional composites construction and the optimized FHMSSs show great potential for future biomedical applications such as drug delivery.

Acknowledgements

This work is supported by the National Natural Science Foundation of China (21301063), Program for New Century Excellent Talents in University (NCET-12-0696), Natural Science Foundation of Education Department of Henan Province (12B150015), Sci-tech Development Programme of Zhengzhou in 2012 (20120325) and Scientists and Technicians Troop Construction Programs of Zhengzhou (131PLJRC649). We thankfully acknowledge N. J. Hao (Technical Institute of Physics and Chemistry, CAS) for his advice on the BET measurement and the cellular experiment.

Notes and references

Institute of Nanostructured Functional Materials, Huanghe Science and Technology College, Zhengzhou, Henan 450006, China. Email: yyggwang@gmail.com

‡ *These authors contribute equally to this article.*

† Electronic Supplementary Information (ESI) available: XRD patterns of the GOs, Graphenes and Si-GQDs, C-NMR spectra of Si-GQDs, the optical photographs of Si-GQDs film and block, PL spectra of the Si-GQDs block, SEM and TEM images of the etched silica spheres without Si-GQDs, TEM images and PL spectra of the FHMSSs with different amount of AEAPTMS, $R_{PL\ retained}$ definition, PL spectra of FHMSSs. See DOI: 10.1039/b000000x/

1. X. Jia, J. Liand E. Wang, *Nanoscale*, 2012, **4**, 5572.
2. Y. Zhang, H. Goncalves, J. C. G. Esteves da Silvaand C. D. Geddes, *Chem. Commun.*, 2011, **47**, 5313.
3. A. B. Bourlinos, A. Bakandritsos, A. Kouloumpis, D. Gournis, M. Krysmann, E. P. Giannelis, K. Polakova, K. Safarova, K. Holaand R. Zboril, *J. Mater. Chem.*, 2012, **22**, 23327.
4. Z. Qian, J. Ma, X. Shan, L. Shao, J. Zhou, J. Chen and H. Feng, *RSC Adv.*, 2013, **3**, 14571.
5. S. Zhu, J. Zhang, C. Qiao, S. Tang, Y. Li, W. Yuan, B. Li, L. Tian, F. Liu, R. Hu, H. Gao, H. Wei, H. Zhang, H. Sun and B. Yang, *Chem. Commun.*, 2011, **47**, 6858.
6. J. Shen, Y. Zhu, X. Yang and C. Li, *Chem. Commun.*, 2012, **48**, 3686.
7. P. C. Hsu, P. C. Chen, C. M. Ou, H. Y. Chang and H. T. Chang, *J. Mater. Chem. B*, 2013, **1**, 1774.
8. V. Gupta, N. Chaudhary, R. Srivastava, G. D. Sharma, R. Bhardwaj and S. Chand, *J. Am. Chem. Soc.*, 2011, **133**, 9960.
9. Y. Li, Y. Hu, Y. Zhao, G. Shi, L. Deng, Y. Hou and L. Qu, *Adv. Mater.*, 2011, **23**, 776.
10. J. Wang, X. Xin and Z. Lin, *Nanoscale*, 2011, **3**, 3040.
11. X. Yan, X. Cui, B. Li and L. Li, *Nano Lett.*, 2010, **10**, 1869.
12. H. Tetsuka, R. Asahi, A. Nagoya, K. Okamoto, I. Tajima, R. Ohta and A. Okamoto, *Adv. Mater.*, 2012, **24**, 5333.
13. H. Li, X. He, Z. Kang, H. Huang, Y. Liu, J. Liu, S. Lian, C. H. A. Tsang, X. Yang and S.T. Lee, *Angew. Chem. Inter. Ed.*, 2010, **49**, 4430.
14. H. Zhang, H. Ming, S. Lian, H. Huang, H. Li, L. Zhang, Y. Liu, Z. Kang and S.T. Lee, *Dalton Trans.*, 2011, **40**, 10822.
15. C. W. Lai, Y. H. Hsiao, Y. K. Peng and P. T. Chou, *J. Mater. Chem.*, 2012, **22**, 14403.
16. L. Li, G. Wu, G. Yang, J. Peng, J. Zhao and J. J. Zhu, *Nanoscale*, 2013, **5**, 4015.
17. L. A. Ponomarenko, F. Schedin, M. I. Katsnelson, R. Yang, E. W. Hill, K. S. Novoselov and A. K. Geim, *Science*, 2008, **320**, 356.
18. L. Bao, Z. L. Zhang, Z. Q. Tian, L. Zhang, C. Liu, Y. Lin, B. Qi and D. W. Pang, *Adv. Mater.*, 2011, **23**, 5801.
19. Y. Li, Y. Zhao, H. Cheng, Y. Hu, G. Shi, L. Dai and L. Qu, *J. Am. Chem. Soc.*, 2012, **134**, 15.
20. Y. Dong, C. Chen, X. Zheng, L. Gao, Z. Cui, H. Yang, C. Guo, Y. Chi and C. M. Li, *J. Mater. Chem.*, 2012, **22**, 8764.
21. J. Shen, Y. Zhu, C. Chen, X. Yang and C. Li, *Chem. Commun.*, 2011, **47**, 2580.
22. P. Russo, A. Hu, G. Compagnini, W. W. Duley and N. Y. Zhou, *Nanoscale*, 2014, **6**, 2381.
23. R. Liu, D. Wu, X. Feng and K. Müllen, *J. Am. Chem. Soc.*, 2011, **133**, 15221.
24. L. Zhi and K. Müllen, *J. Mater. Chem.*, 2008, **18**, 1472.
25. M. L. Mueller, X. Yan, B. Dragnea and L. Li, *Nano Lett.*, 2011, **11**, 56.
26. D. Pan, J. Zhang, Z. Li and M. Wu, *Adv. Mater.*, 2010, **22**, 734.
27. Q. Xue, H. Huang, L. Wang, Z. Chen, M. Wu, Z. Li and D. Pan, *Nanoscale*, 2013, **5**, 12098.
28. F. Jiang, D. Chen, R. Li, Y. Wang, G. Zhang, S. Li, J. Zheng, N. Huang, Y. Gu, C. Wang and C. Shu, *Nanoscale*, 2013, **5**, 1137.
29. J. Shen, Y. Zhu, X. Yang, J. Zong, J. Zhang and C. Li, *New J. Chem.*, 2012, **36**, 97.
30. Z. L. Wu, M. X. Gao, T. T. Wang, X. Y. Wan, L. L. Zheng and C. Z. Huang, *Nanoscale*, 2014, **6**, 3868.
31. P. Luo, Z. Ji, C. Li and G. Shi, *Nanoscale*, 2013, **5**, 7361.
32. Q. Tang, Z. Zhou and Z. Chen, *Nanoscale*, 2013, **5**, 4541.
33. G. S. Kumar, R. Roy, D. Sen, U. K. Ghorai, R. Thapa, N. Mazumder, S. Saha and K. K. Chattopadhyay, *Nanoscale*, 2014, **6**, 3384.
34. F. Wang, Z. Xie, H. Zhang, C. Liu and Y. Zhang, *Adv. Funct. Mater.*, 2011, **21**, 1027.
35. Y. P. Sun, B. Zhou, Y. Lin, W. Wang, K. A. S. Fernando, P. Pathak, M. J. Meziani, B. A. Harruff, X. Wang, H. Wang, P. G. Luo, H. Yang, M. E. Kose, B. Chen, L. M. Veca and S. Y. Xie, *J. Am. Chem. Soc.*, 2006, **128**, 2.
36. Z. Xie, F. Wang and C. Liu, *Adv. Mater.*, 2012, **24**, 1716.
37. P. C. Chen, Y. N. Chen, P. C. Hsu, C. C. Shih and H. T. Chang, *Chem. Commun.*, 2013, **49**, 1639.
38. B. P. Biswal, D. B. Shinde, V. K. Pillai and R. Banerjee, *Nanoscale*, 2013, **5**, 10556.
39. D. C. Marcano, D. V. Kosynkin, J. M. Berlin, A. Sinitskii, Z. Sun, A. Slesarev, L. B. Alemany, W. Lu, and J. M. Tour, *ACS nano*, 2010, **4**, 4806.
40. D. Chen, L. Li, F. Tang and S. Qi, *Adv. Mater.*, 2009, **21**, 3804.
41. X. Fang, C. Chen, Z. Liu, P. Liu and N. Zheng, *Nanoscale*, 2011, **3**, 1632.
42. H. Blas, M. Save, P. Pasetto, C. Boissière, C. Sanchez and B. Charleux, *Langmuir*, 2008, **24**, 13132.
43. S. Kumari and P. D. Sahare, *J. Mater Sci. Technol.*, 2013, **29**, 742.
44. L. Du, S. J. Liao, H. A. Khatib, J. F. Stoddart and J. I. Zink, *J. Am. Chem. Soc.*, 2009, **131**, 15136.
45. Y. F. Zhu, T. Ikoma, N. Hanagata and S. Kaskel, *Small*, 2010, **6**, 471.
46. Q. Zhang, T. R. Zhang, J. P. Ge and Y. D. Yin, *Nano Lett.*, 2008, **8**, 2867.
47. W. Cai, I. R. Gentle, G. Q. Lu, J. J. Zhu and A. Yu, *Anal. Chem.*, 2008, **80**, 6.
48. J. Lee, J. C. Park, J. U. Bang and H. Song, *Chem. Mater.*, 2008, **20**, 5839.

Graphical Abstract:

We demonstrate an affordable method to fabricate organosilane-functionalized graphene quantum dots and their encapsulation into bi-layer hollow silica spheres for bioimaging application.